Sustainable Food Technology

ROYAL SOCIETY OF CHEMISTRY

PAPER

View Article Online
View Journal

Cite this: DOI: 10.1039/d5fb00748h

Pulsed electric field pretreatment reveals matrix-dependent mass transfer mechanisms in phenolic recovery from pomegranate peel

Gessica Maria Lopes Faria and Eric Keven Silva *

Understanding the mechanisms that govern mass transfer is crucial for designing efficient and sustainable extraction processes for plant-derived bioactive compounds. Pulsed electric fields (PEF) pretreatment is widely recognized for enhancing extraction by inducing electroporation and disrupting cell structures. However, its effectiveness is highly dependent on matrix characteristics and is often overestimated in systems with high solute availability. In this study, PEF was applied as a pretreatment step prior to pressurized liquid extraction (PLE) to improve mass transfer during phenolic recovery from fresh pomegranate peel, a matrix intrinsically rich in phenolic compounds. Despite achieving significant cell permeabilization ($Z > 0.9$), PEF resulted in only marginal improvements in extraction yield, suggesting that diffusion driven by the chemical potential difference between the matrix and the solvent was the dominant mechanism. To clarify the underlying mass transfer phenomena, stirred liquid extraction (SLE) and ultrasound-assisted extraction (UAE) were performed as comparative strategies, allowing the relative contributions of solvent accessibility, diffusional driving force, and structural disruption to be systematically evaluated. Kinetic modeling using Peleg's equation and cumulative solvent-to-feed (S/F) analysis revealed that more than 80% of phenolics were recovered within the first 5 min of batch extraction, and that increasing solvent availability minimized acoustic cavitation-related effects. These findings demonstrate that PEF effectiveness is strongly matrix-dependent and provide critical mechanistic insights for the rational design of mass transfer–intensifying strategies, enabling more efficient and scalable phenolic recovery from agro-industrial by-products.

Received 27th October 2025
Accepted 23rd February 2026

DOI: 10.1039/d5fb00748h

rsc.li/susfoodtech

Sustainability spotlight

This study provides crucial mechanistic insights to design energy-efficient and resource-minimal processes for valorizing agro-industrial by-products, specifically fresh pomegranate peel. We demonstrate that the effectiveness of PEF pretreatment is strongly matrix-dependent and did not significantly enhance phenolic recovery in solute-rich systems, where over 80% of phenolics are recovered rapidly *via* diffusion. By showing that solvent accessibility, not structural disruption, is the dominant factor, this work enables the rational design of extraction strategies that reduce energy consumption (by avoiding unnecessary high-energy pretreatments) and maximize value recovery (*via* highly efficient methods such as pressurized liquid extraction). This approach supports a circular bioeconomy by turning waste into high-value ingredients with a demonstrated low environmental footprint, prioritizing efficiency for scalable and sustainable food technology.

1. Introduction

Pomegranate peel is recognized as a rich source of phenolic compounds, which are associated with relevant biological effects such as improvement of oxidative stress, reduction of inflammatory processes, and activation of antioxidant enzymes.[1] In recent years, several studies have sought to improve the extraction of these metabolites, not only in terms of yield but also by considering the adoption of cleaner and more sustainable processes.[2–4] Pomegranate peel stands out not only for its high abundance as a by-product but also for its exceptionally elevated levels of free phenolic compounds, which are markedly higher than those of most commonly valorized agro-residues.[5] While residues such as potato peel typically contain 48–821 mg GAE/100 g and grape pomace ranges from 5.4–10.7 g GAE/100 g, pomegranate peel frequently exceeds 6.3–20.8 g GAE/100 g and is among the richest natural sources of hydrolyzable tannins, especially punicalagin.[5–7] This unusually high phenolic availability creates a steep intrinsic concentration gradient during extraction, making pomegranate peel an ideal model to investigate matrix-dependent mass transfer phenomena.

Universidade Estadual de Campinas (UNICAMP), Faculdade de Engenharia de Alimentos (FEA), Rua Monteiro Lobato, 80, Campinas, SP CEP: 13083-862, Brazil. E-mail: ekeven@unicamp.br

Nevertheless, the extraction process is complex, as mass transfer during extraction comprises four main steps: (i) solvent penetration into the solid particle; (ii) dissolution of the solute into the solvent inside the particle; (iii) diffusion of the dissolved solute to the particle surface; and (iv) diffusion of the dissolved solute into the external solvent.[8] The diffusion of the solute into the extracting medium is generally considered the rate-limiting step. The rate at which compounds dissolve and reach equilibrium in the liquid phase is influenced by parameters such as temperature, agitation intensity, particle size, and solvent selection.[9–11]

In this scenario, emerging extraction technologies, such as high-intensity ultrasound (HIUS), microwave heating, and pressurized liquid extraction (PLE), have been widely employed to overcome mass transfer limitations, reduce energy consumption, and minimize solvent usage. In parallel, pulsed electric fields (PEF) have attracted increasing attention not as an extraction technique itself, but as a pretreatment strategy capable of enhancing the subsequent extraction steps.[12] PEF is a non-thermal process that promotes electroporation, increasing cell membrane permeability and facilitating solute release.[13] Moreover, PEF can also be integrated into different biorefinery schemes and combined with extraction-assisted techniques, such as HIUS or PLE, to intensify compound recovery in a complementary manner.

PEF involves the application of short, high-intensity electric pulses that induce electroporation, *i.e.*, the formation of aqueous pores in cell membranes. This phenomenon markedly increases membrane permeability and disrupts structural barriers, thereby facilitating solvent access to intracellular domains and enhancing ion and molecule diffusivity. In this sense, PEF does not act as an extraction technique *per se*, but rather as a pretreatment designed to overcome the physical resistance of the plant matrix, a critical step that determines how easily mass transfer can occur during subsequent extraction.[14–16] In contrast, high-intensity ultrasound (HIUS) is itself an extraction technology. Its action is primarily mechanical, driven by acoustic cavitation, a phenomenon involving the formation, growth, and violent collapse of microbubbles within the liquid medium. These implosions generate intense localized shear forces and microjets, while also inducing sonoporation (the formation of transient pores in cell structures) and creating microturbulence and localized temperature increases. Together, these effects promote deeper solvent penetration, accelerate solute diffusion, and significantly enhance the overall extraction kinetics.[17–19]

Recent studies have demonstrated that PEF pretreatment can enhance the extraction of bioactive compounds from a variety of plant matrices, including olive leaves, grape residues and pomace, and brewer's spent grains, often resulting in substantial increases in phenolic content and antioxidant activity, along with reductions in extraction time and solvent consumption.[20–23] The performance of PEF is highly dependent on both operational parameters and the intrinsic characteristics of the raw material, such as electrical conductivity, pH, cell wall composition, and structural complexity.[24] This matrix dependence highlights the need for case-by-case evaluation, since the mechanisms governing extraction can vary considerably. In particular, when the native structure of the biomass already allows for rapid solvent penetration or when the solute concentration is intrinsically high, electroporation may no longer be the limiting factor. Instead, other mechanisms, such as the chemical potential difference between the matrix and the solvent, may dominate the extraction kinetics.[25]

In this context, our study focuses precisely on exploring these mechanistic boundaries. We applied PEF as a pretreatment to fresh pomegranate peel prior to PLE, aiming to increase mass transfer by disrupting physical barriers.[26–28] However, only a marginal enhancement in phenolic recovery was observed, suggesting that the high phenolic content of pomegranate peel may itself establish a steep diffusion driving force, thereby reducing the relative contribution of electroporation. Understanding this interplay between matrix composition, pretreatment effects, and mass transfer mechanisms is essential for designing more efficient and targeted extraction strategies.

To investigate this hypothesis, we designed a comprehensive experimental approach aimed at dissecting the relative contributions of different mass transfer mechanisms in phenolic extraction from pomegranate peel. Comparative extractions were performed using stirred liquid extraction (SLE), ultrasound-assisted extraction (UAE), and PLE, each representing distinct mass transfer-intensifying conditions. Kinetic modeling based on Peleg's equation, cumulative solvent-to-feed mass ratio (S/F) analysis, and a sustainability assessment using the Path2Green framework were integrated to provide a multidimensional understanding of the extraction behavior. By systematically examining how solute availability, structural resistance, and solvent accessibility interact, this study aims to elucidate the mechanistic boundaries of PEF pretreatment effectiveness and reveal the conditions under which diffusion-driven phenomena outweigh electroporation effects. Such insights are fundamental for the rational design of efficient, low-energy, and sustainable extraction processes, ultimately enhancing the industrial potential of pomegranate peel valorization.

2. Material and methods

2.1 Raw material and sample preparation

Pomegranate (*Punica granatum* L.) of the "Wonderful" cultivar, grown in Peru, were purchased from a local market in Campinas, São Paulo, Brazil. The fruits were washed, sanitized, and manually peeled. Fresh peels intended for PEF experiments were stored under refrigeration and protected from light. In parallel, other peels were dried in a forced-air circulation oven at 50 °C for 24 h. Subsequently, the dried material was ground in a blender (MX 15000, Waring Commercial Inc., McConnellsburg, USA) under standardized power settings (60%) in three intervals of 10 s, resulting in a pomegranate peel flour.

Particle size distribution of the pomegranate peel flour was determined using a vibratory sieve shaker with sequential mesh sizes of 9, 12, 16, 24, 48, and 80 mesh (equivalent to the Tyler series, Wheeling, USA). The mean particle diameter was calculated according to ASAE and U. Committee.[29] The particle size

ranged from 0.18 to 2.00 mm, with a mean particle diameter of 0.556 mm. For the extraction processes, fractions corresponding to 16, 24, and 48 mesh were selected, as they represented approximately 55% of the total flour mass and were within the central range of the particle size distribution. Accordingly, the particle size of the selected fractions ranged from 0.297 to 1.00 mm, with a mean particle diameter of 0.727 mm.

2.2 PEF pretreatment applied to fresh pomegranate peel

Experiments were conducted using fresh pomegranate peel residues to evaluate the effect of PEF pretreatment on the extraction of phenolic compounds by PLE. A commercial PEF system (Vitave, Prague, Czech Republic) capable of delivering monopolar square-wave pulses of up to 10 kV was employed, equipped with a cylindrical treatment chamber with an electrode gap of 3 cm. Treatment parameters were set as follows: electric field intensity of 1 kV cm^{-1}, pulse frequency of 1 Hz, pulse duration of 10 μs, and number of pulses ranging from 5 to 40. Fresh peels were comminuted, and 10 g of sample were weighed and transferred to the treatment chamber. Subsequently, 110 mL of distilled water was added, the initial conductivity was measured, and PEF treatments were applied accordingly.

The degree of cell membrane permeabilization induced by PEF was evaluated by calculating the cell disintegration index (Z), which quantifies the extent to which the electrical treatment disrupts the cell structure based on changes in electrical conductivity before and after treatment. The parameter ranges from 0 to 1, where $Z = 0$ indicates no electroporation (intact tissue) and $Z = 1$ represents complete cell disintegration. The Z index was calculated following the methodology described by Rastorhuiev *et al.*[30] using eqn (1). Electrical conductivity was considered maximal after 100 additional pulses were applied and no further significant changes were observed.

The specific energy input corresponding to each pulse number was calculated according to eqn (2), which expresses the total specific energy (W_t) delivered to the sample during PEF treatment based on the electrical parameters and system geometry.[14]

$$Z = \frac{(\sigma - \sigma_i)}{(\sigma_{max} - \sigma_i)} \quad (1)$$

where: σ = electrical conductivity of the sample after the PEF treatment σ_i = initial electrical conductivity of the sample σ_{max} = maximum electrical conductivity of the sample

$$W_t = \frac{U^2 \times n \times \tau \times \sigma_i \times A}{m \times L} \quad (2)$$

where: W_t = total specific energy (J kg^{-1}) U = voltage (V) n = number of pulses τ = pulse duration (s) σ_i = initial electrical conductivity of the sample A = electrode area (m^2) m = sample mass subjected to PEF (kg) L = distance between electrodes (m).

After identifying the optimal specific energy input, that is, the condition yielding a Z index close to 1, PLE experiments were conducted. The solvent system consisted of a water/ethanol mixture (1 : 1, v/v), under the same operational conditions described in Section 2.2.2. Extract fractions were collected at the following time intervals (min): 2.5, 5, 10, 15, 20, 25, and 30, corresponding to a total S/F ratio of approximately 27. Control extractions using PLE system without PEF pretreatment were also carried out. All extractions were performed in duplicate.

2.3 Kinetics of phenolic compounds extraction from pomegranate peel flour

Extraction kinetics of pomegranate peel flour were investigated using three different methods: stirred liquid extraction (SLE), ultrasound-assisted extraction (UAE), and pressurized liquid extraction (PLE).

2.3.1 Kinetics of stirred liquid and ultrasound-assisted extraction. For both SLE and UAE kinetics, the experiments were carried out using a custom system composed of a beaker, a metal apparatus, and a filter cloth. In each run, 3 g of pomegranate peel by-product flour were combined with an ethanol–water mixture (1 : 1, w/w) in volumes sufficient to achieve the desired solid-to-solvent ratio (S/F = 5, 10, or 30). Samples were collected at the following time intervals (min): 0.5, 1, 2, 3, 4, 5, 7.5, 10, 15, 20, 25, 30, 40, 50, and 60. The flour remained in the extraction apparatus throughout the experiment, enabling successive solvent replacement for extract recovery. After each interval, the extract was filtered and stored, and fresh solvent was added according to each S/F evaluated. Therefore, in sequential extractions denoted as S/F (n by n), where n represents the solvent-to-feed mass ratio (n = 5, 10, or 30), the solvent was replaced according to the selected S/F ratio, maintaining the same solvent volume relative to the solid mass at each extraction time. Extract volumes were recorded and used to calculate the phenolic compound concentration in the samples. Kinetic curves were constructed from the cumulative phenolic content determined at each collection point. All experiments were performed in duplicate for each experimental condition of S/F investigated.

For SLE kinetics, the systems were maintained under magnetic stirring (500 rpm) at 40 °C using a magnetic stirrer (MR HEI-TEC Ø145, Heidolph, Schwabach, DEU). For UAE kinetics, the systems were subjected to ultrasonic probe treatment at 20 kHz frequency, maximum power of 750 W, and probe diameter of 13 mm (VCX 750, Sonics & Materials, Inc., Newtown, United States). The applied amplitude was set to 75%, corresponding to an acoustic power of 43.01 ± 0.2 W.[31]

2.3.2 Pressurized liquid extraction kinetics. PLE was performed using a system consisting of a solvent reservoir, an HPLC pump (PU-2080, Jasco corporation, Tokyo, Japan), a pressure gauge, and an extraction vessel connected to a temperature controller and housed in an electrically heated jacket. Two shut-off valves and a backpressure valve maintained constant operating pressure. All connections were made using 1/16″ and 1/8″ stainless steel tubing.[28]

The extraction vessel was loaded with 3 g of pomegranate peel by-product flour, packed between cotton layers at both ends to prevent preferential channeling. An ethanol–water mixture (1 : 1, v/v) was used as the solvent, with a total solid-to-

liquid ratio fixed at 100. The extraction was conducted at 40 °C, 100 bar, and a constant flow rate of 3 mL min^{-1}. Initially, the system was heated to the target temperature and pressurized with the outlet closed, allowing a 10 min static extraction for system equilibration. After this period, the valves were opened and adjusted to maintain pressure, initiating the dynamic extraction phase.

Extract fractions were collected at the following time intervals (min): 2.5, 5, 7.5, 12.5, 17.5, 22.5, 27.5, 37.5, 47.5, 57.5, 67.5, 77.5, 87.5, 97.5, and 107.5. The mass and volume of each fraction were recorded, and the extracts were stored for later analysis. Kinetic curves were constructed from cumulative phenolic content at each collection point. Duplicate kinetic curves were obtained under the same operating conditions.

2.4 Total phenolic content analysis

The extracts obtained at each time point of the kinetic experiments were analyzed for total phenolic content (TPC) using the Folin-Ciocalteu method, as described by Singleton and Rossi.[32] All analyses were performed in triplicate. Briefly, 25 μL of the appropriately diluted sample, 25 μL of Folin-Ciocalteu reagent (1 : 1, v/v), and 200 μL of sodium carbonate solution (5%, w/v) were added to the wells of a microplate. The reaction mixture was kept in the dark at room temperature for 20 min, and absorbance was measured at 760 nm using a spectraMax Mini microplate reader (Molecular Devices, USA). The blank consisted of 25 μL of distilled water instead of the sample. A calibration curve prepared with gallic acid (5–80 μg mL; $R^2 = 0.995$) was used for quantification. Results were expressed as milligrams of gallic acid equivalents (mg GAE) per gram of pomegranate peel flour (mg GAE per g).

2.5 Extraction kinetics modeling using the peleg equation

Mathematical models are widely employed to facilitate the optimization, simulation, design, and control of processes, as well as to improve the efficiency of energy, time, and solvent usage. The Peleg model is a classical empirical hyperbolic equation originally developed to describe moisture sorption curves. Owing to the similarity between the shapes of sorption and extraction curves, this model has been adapted and extensively applied to describe solid–liquid extraction processes for metabolites such as phenolic compounds.[33]

Experimental data obtained from the extraction kinetics of phenolic compounds using SLE, UAE, and PLE were fitted to the Peleg kinetic model.[34] Two kinetic parameters were determined according to the original model proposed by Peleg for sorption kinetics (eqn (3)).

$$C(t) = C_0 + \frac{t}{K_1 + K_2\, t} \tag{3}$$

where: t (min) = extraction time $C(t)$ = extraction yield at time t (mg GAE per g pomegranate peel flour) C_0 = initial extraction yield at $t = 0$ (mg GAE per g pomegranate peel flour) K_1 = constant related to the initial extraction rate (min g flour per mg GAE) K_2 = capacity constant, which governs the approach of the yield toward its maximum value (g flour per mg GAE).

The reciprocal value of K_1 corresponds to the initial extraction rate constant B_0 (mg GAE per g flour min) at $t = 0$ (eqn (4)). Similarly, the reciprocal value of K_2 allows the determination of the equilibrium yield concentration ($t \rightarrow \infty$), or maximum extraction capacity, C_e (mg GAE per g flour) (eqn (5)). The kinetic constants K_1 and K_2, as well as the estimate of C_0, were determined using *R* statistical software.

$$\frac{dC(t)}{dt} = \frac{1}{K_1} = B_0 \tag{4}$$

$$C_e = C_0 + \frac{1}{K_2} \tag{5}$$

The quality of fit between experimental data and the model was evaluated using the root mean square error (RMSE) and the standard deviation of residuals (σ). RMSE (eqn (6)) was used to estimate the average deviation between predicted and observed values, indicating the accuracy of the model. The parameter σ was used to assess the consistency of the model by measuring the dispersion of residuals around the regression line.

$$\mathrm{RMSE} = \sqrt{\sum_{i=1}^{n} \frac{(y_i - \hat{y}_i)^2}{n}} \tag{6}$$

where: y_i = observed value (experimental) $\hat{y}_i$ = value predicted by the model n = total number of experimental points $(y_i - \hat{y}_i)$ = residual at each point.

2.6 Preparation of representative extracts

Representative extracts from the duplicate extraction kinetics of SLE S/F (10 by 10) and UAE S/F (10 by 10) were prepared for subsequent analyses of phenolic compound quantification by liquid chromatography, total phenolic content, and antioxidant activity. The selection of SLE and UAE kinetics with an S/F ratio of 10 was based on achieving the same total S/F ratio of 100 as in the PLE kinetics. Accordingly, the first 10 points from the SLE S/F (10 by 10) and UAE S/F (10 by 10) kinetics were used to prepare representative extracts, while all 15 points were used for PLE. For the calculations, the final volumes up to the defined number of points and the volume of each collection point were considered. The percentage contribution of each point to the total volume was then calculated. Based on these percentages, a smaller total volume (3 mL) of the representative extract was prepared, maintaining the proportional contribution of each collection point.

2.7 Chromatographic analysis of phenolic compounds in representative extracts

Phenolic compounds in the samples were determined using a Dionex UltiMate 3000 system (Thermo Fisher Scientific, Waltham, MA, USA) equipped with a diode array detector, following the method developed and validated by Borsoi *et al.*[35] Separation was carried out on an Acclaim™ 120 Å C18 column (250 × 4.6 mm i.d., 5 μm particle size; Thermo Fisher Scientific, Waltham, MA, USA) at a flow rate of 0.5 mL min^{-1} under a gradient elution program. The column temperature was maintained at

32 °C, and the injection volume was 20 μL. The mobile phases consisted of 0.1% (v/v) formic acid in deionized water (Eluent A) and HPLC-grade acetonitrile (Eluent B). The gradient program was as follows: 0–5 min, 5% B; 5–27 min, 5–29% B; 27–33 min, 35% B; 33–38 min, 95% B; and 38–48 min, 5% B. Chromatograms were recorded simultaneously at 260, 320, 360, and 520 nm. Phenolic compounds were identified by comparing retention times and UV-vis spectra with those of analytical standards. Quantification was performed using calibration curves prepared from commercial standards, and results were expressed as micrograms per milliliter of sample (μg mL^{-1}).

2.8 TPC and antioxidant activity assays for representative extracts

2.8.1 Total phenolic content (TPC). The TPC of representative extracts was determined as described in Section 2.3. Results were expressed as μg GAE per mL.

2.8.2 Trolox equivalent antioxidant capacity (TEAC) assay. The TEAC assay was performed according to Re *et al.*,[36] with slight modifications, and all analyses were conducted in triplicate. The $ABTS^{\bullet+}$ radical cation was generated by mixing 5 mL of ABTS solution (7 mM in water) with 88 μL of potassium persulfate solution (140 mM) and storing the mixture in the dark for 16 h. The working solution for sample analysis was obtained by diluting the $ABTS^{\bullet+}$ solution with ultrapure water to an absorbance of 0.70 ± 0.02 at 734 nm. For each assay, 40 μL of diluted sample was mixed with 200 μL of the $ABTS^{\bullet+}$ working solution in a microplate well and incubated for 6 min at room temperature. The absorbance of the remaining $ABTS^{\bullet+}$ was measured at 734 nm against a blank (240 μL of distilled water) using a SpectraMax Mini microplate reader (Molecular Devices, USA). A calibration curve prepared with Trolox (5–150 μmol L; $R^2 = 0.996$) was used to quantify antioxidant capacity. Results were expressed as μmol Trolox equivalents (TE) per milliliter of sample (μmol TE mL^{-1}).

2.8.3 Ferric reducing antioxidant power (FRAP) assay. The FRAP assay was conducted as described by Benzie and Strain,[37] with slight modifications, and all analyses were performed in triplicate. The FRAP reagent was prepared fresh by mixing 300 mM acetate buffer (pH 3.6), 10 mM TPTZ (2,4,6-tripyridyl-*s*-triazine) in 40 mM HCl, and 20 mM ferric chloride in a 10 : 1 : 1 (v/v/v) ratio. For the assay, 20 μL of sample was added to a microplate well containing 180 μL of FRAP reagent and 60 μL of distilled water. After incubation at 37 °C for 30 min, the absorbance was measured at 593 nm using a SpectraMax Mini microplate reader (Molecular Devices, USA). A calibration curve prepared with Trolox (25–400 μmol L; $R^2 = 0.993$) was used for quantification. Results were expressed as μmol TE mL^{-1}.

2.9 Scanning electron microscopy (SEM)

Morphological images of the biomass obtained after phenolic compound extraction from the SLE S/F (10 by 10), UAE S/F (10 by 10), and PLE kinetic experiments were acquired using a scanning electron microscope (Hitachi TM4000Plus, Tokyo, Japan). Samples were observed without gold coating at a magnification of 300×, using an electron beam with an accelerating voltage of 10 kV under vacuum conditions.

2.10 Sustainability evaluation of the extraction processes *via* Path2Green metric

The sustainability of SLE, UAE, and PLE was assessed using the Path2Green metric,[38] which scores the twelve updated principles of green extraction (biomass, transport, pretreatment, solvent, scaling, purification, yield, post-treatment, energy, application, repurposing, and waste management) on a scale from −1 to 1. Higher scores indicate greater alignment with sustainable practices.

2.11 Statistical analysis

The results are presented as mean values with their corresponding standard deviations. Extraction kinetics plots using raw data were constructed from the mean values and actual deviations. For Peleg model fitting, the mean values of duplicate kinetic curves were used, and deviations were estimated by the root mean square error (RMSE) and the residual standard deviation (σ). Differences among the data presented in Sections 2.6 and 2.7 were evaluated by analysis of variance (ANOVA) using Minitab 18 software, and means were compared by Tukey's test at a significance level of p-value ≤ 0.05.

3. Results and discussion

3.1 Effect of PEF pretreatment on phenolic compound extraction from fresh pomegranate peel

Fresh pomegranate peel was selected as the raw material for PEF pretreatment because the structural integrity of the biological tissue, including intact cell membranes and cell walls, is essential for accurately assessing the electroporation effect. In dried and ground materials, cells are already disrupted due to dehydration and mechanical fragmentation, which significantly reduces the structural resistance to mass transfer and masks the contribution of PEF-induced permeabilization. Therefore, using fresh biomass allows a clearer evaluation of how PEF overcomes natural physical barriers and facilitates solvent access prior to extraction.[15,16]

Fig. 1 presents the cell disintegration index (Z) determined from electrical conductivity measurements before and after PEF treatments at different levels of specific energy input. The fact that the peels had been previously comminuted contributed to a relatively high initial Z value. Upon applying 0.315 kJ kg^{-1}, Z reached 0.97, indicating almost complete cell disintegration. Therefore, the PEF pretreatment conditions were set at 1 kV cm^{-1}, 1 Hz, a pulse duration of 10 μs, and 40 pulses, corresponding to a total specific energy of 0.315 kJ kg^{-1}.

Approximately half of the total phenolic compounds recovered after PLE were released during the initial immersion stage of the comminuted fresh peel, both in the untreated and in the PEF-pretreated samples. This suggests that diffusion driven by the concentration gradient was sufficient to induce an intense extraction, even without the additional contribution of electrical permeabilization. Fig. 2 shows the kinetic profiles of

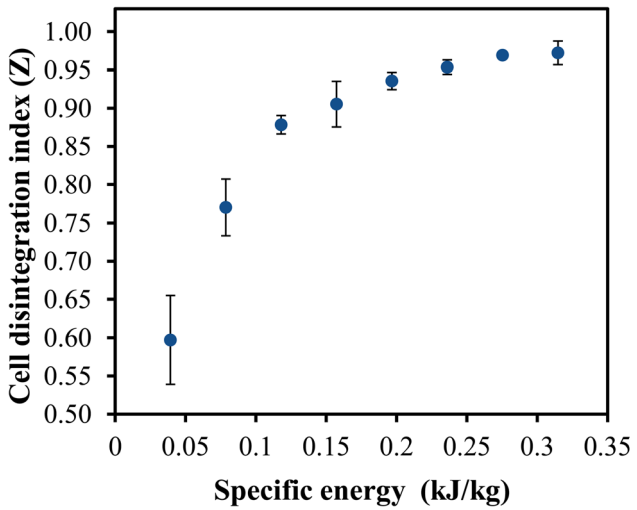

Fig. 1 Cell disintegration index (Z) of fresh pomegranate peel subjected to different levels of specific energy input during PEF pretreatment. PEF: pulsed electric field.

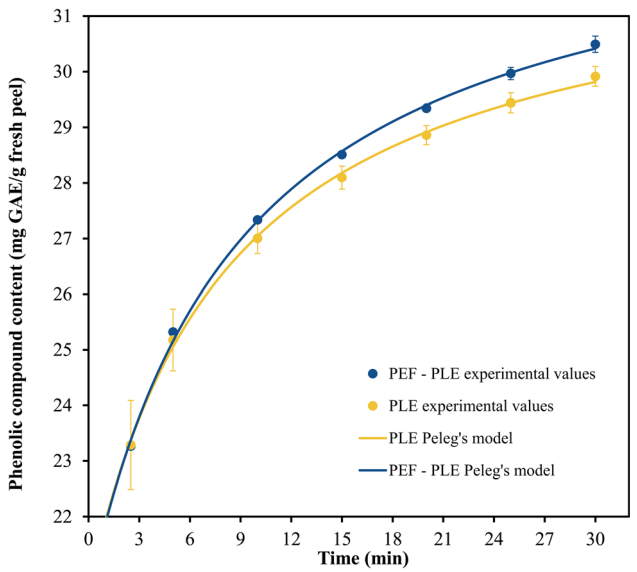

Fig. 2 Kinetic profiles of phenolic compound extraction from fresh pomegranate peel by PLE with and without PEF pretreatment. PLE: pressurized liquid extraction, PEF: pulsed electric field.

phenolic compound extraction, which were nearly superimposed, indicating no significant differences in either the maximum extraction capacity (C_e) or the initial extraction rate (B_0) relative to PLE without PEF pretreatment (Table 1).

Few studies have applied PEF for the recovery of phenolic compounds from pomegranate peel. Significant improvements were reported in aqueous extraction assisted by PEF at 10 kV cm^{-1} and 90–100 kJ kg^{-1} of specific energy, achieving approximately eightfold higher recovery compared with the conventional method.[4] However, the specific energy used was more than 285 times higher than that applied in the present study, and PEF was employed as an extraction-assisting method with a long treatment duration (7 min), rather than as a pretreatment. The combination of PEF and ultrasound has also been investigated for the extraction of phenolic compounds from pomegranate peel. However, the absence of direct comparison with the individual techniques makes it difficult to assess the specific contribution of the electrical step.[39]

For other agri-food residues, the performance of PEF as a pre-treatment has been more evident. In cherry pomace, PEF pre-treatment promoted higher release (~80%) of total bioactive compounds during the first extraction stage. The combined PEF-UAE process led to overall increases of 293% (TPC), 304% (FC), 380% (TAC), and 274% (FRAP) compared with the control.[40] In aromatic herbs of the Lamiaceae family, PEF enhanced the phenolic content and antioxidant activity of thyme, whereas for rosemary, under the same experimental conditions, no significant differences were observed for TPC and FRAP. The lower Z values reported for rosemary confirm its lower degree of electroporation, consistent with its more lignocellulosic structure and higher resistance to cell wall rupture.[25]

PEF was also applied as a pretreatment to evaluate the extraction kinetics of phenolic compounds from potato peel. The pre-treatment increased polyphenol recovery by approximately 10% and reduced the extraction time from 240 to 144 min to reach a yield of 1.06 mg GAE per g.[41] However, the overall kinetic profile remained unchanged, showing a rapid initial release followed by a plateau.

These contrasts show that the effectiveness of PEF is strongly dependent on the characteristics of the plant matrix. Pomegranate peel contains much higher concentrations of free phenolic compounds than other residues (approximately 30 times more than potato peel), which favors a faster, diffusion-controlled extraction. In addition, prior comminution resulted in high initial Z values, reducing the incremental effect of electroporation.

From a mechanistic standpoint, the results indicate that the concentration gradient is the main driving force governing the extraction of phenolic compounds from pomegranate peel. Even when membrane permeability is maximized (Fig. 1), the

Table 1 Kinetic parameters of phenolic compound extraction by PLE and PEF-pretreated PLE, estimated using the Peleg model

Method	K_1 estimate[a]	K_2 estimate[b]	R^2	RMSE	Sigma	B_0[c]	C_e[d]
PEF-PLE	0.70675	0.07837	0.999	0.08	0.11	1.41	32.86
PLE	0.71529	0.08563	0.999	0.08	0.10	1.40	31.86

[a] K_1: constant related to the initial extraction rate (min g fresh peel per mg GAE). [b] K_2: capacity constant, which governs the approach of the yield toward its maximum value (g fresh peel per mg GAE). [c] B_0: initial extraction rate constant at $t = 0$ (mg GAE per g fresh peel min). [d] C_e: maximum extraction capacity (mg GAE per g fresh peel). PLE: pressurized liquid extraction; PEF: pulsed electric field.

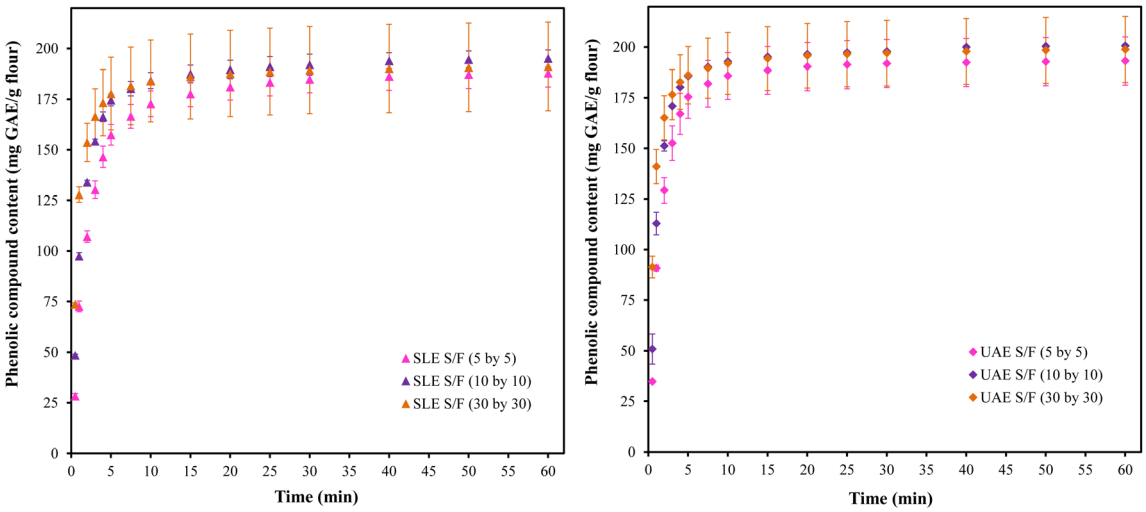

Fig. 3 Comparison of complete extraction kinetics at S/F ratio of 5, 10, and 30 for SLE and UAE. S/F: solvent/feed mass ratio; SLE: stirred liquid extraction; UAE: ultrasound-assisted extraction.

process tends to converge toward an equilibrium recovery similar to the untreated if the initial concentration gradient is already sufficiently steep. To investigate this hypothesis, additional conditions were evaluated using dried and finely milled peel to reduce diffusion resistance and better isolate the effect of the concentration gradient. Under these conditions, mass transfer was facilitated, allowing clearer assessment of the diffusion-driven process while minimizing structural barriers associated with intact cellular matrices.

3.2 Kinetic profiles of phenolic compound recovery from pomegranate peel flour

The extraction kinetics of phenolic compounds from pomegranate peel flour at S/F ratio of 5, 10, and 30 over 60 min for both SLE and UAE are shown in Fig. 3. For all extraction methods and S/F ratios, more than 80% of total phenolics were recovered within the first 5 minutes, indicating that extraction is dominated by an initial rapid diffusion stage. Regardless of the extraction method, increasing the S/F ratio enhanced the initial recovery rate during the early stages of the process. However, once the plateau in phenolic content was approached, further increases in S/F no longer influenced the extraction outcome, resulting in similar total phenolic yields across the tested S/F ratios. Furthermore, the maximum recovery of phenolic compounds was reached rapidly, indicating that a 60 min processing time was unnecessary.

To quantify the observations and compare extraction dynamics across methods, the data were dimensionless according to eqn (7), and new curves were generated (Fig. 4). This dimensionless transformation enhances the visualization of kinetic differences and extraction rates, particularly given that maximum phenolic yields were similar across processes. Similar dimensionless strategies have been widely applied in drying kinetics,[42] in employing dimensionless groups to elucidate heat and mass transfer mechanisms,[43] and in modeling phenolic extraction process.[10]

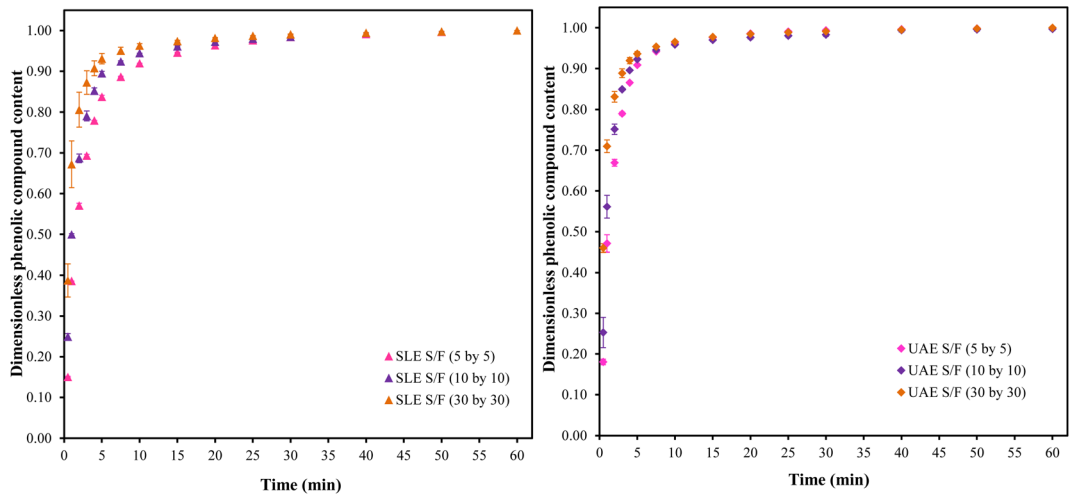

Fig. 4 Comparison of complete dimensionless extraction kinetics at S/F ratio of 5, 10, and 30 for SLE and UAE. S/F: solvent/feed mass ratio; SLE: stirred liquid extraction; UAE: ultrasound-assisted extraction.

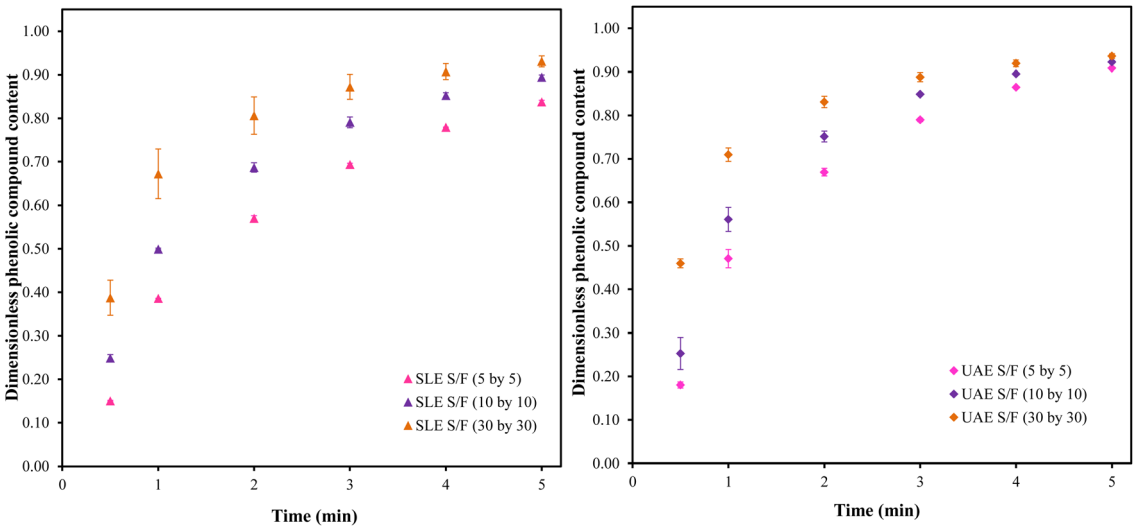

Fig. 5 Comparison of the first 5 min of dimensionless extraction kinetics at S/F ratio of 5, 10, and 30 for SLE and UAE. S/F: solvent/feed mass ratio; SLE: stirred liquid extraction; UAE: ultrasound-assisted extraction.

$$C^*(t) = \frac{C(t)}{C_f} \quad (7)$$

where: $C(t)$ = the dimensionless concentration at time t $C(t)$ = the phenolic concentration at time t (mg GAE per g flour) C_f = the final concentration (mg GAE per g flour).

The extraction curves showed a clear distinction between the initial and subsequent stages of mass transfer. Based on this early extraction pattern, in which over 80% of the total recovery takes place within the first 5 min, the dimensionless kinetics were re-examined by focusing solely on this initial period (Fig. 5). This approach allowed a clearer assessment of the influence of increasing S/F. An increase in the S/F ratio enhanced phenolic recovery, which can be attributed to the greater chemical potential driving force.

The chemical potential difference between the solute within the solid matrix and in the surrounding solution is the driving force for the extraction process. In practical terms, this potential difference can be assessed through the concentration gradient, with the mass transfer rate expressed as the product of the difference between the external solute concentration and the solute concentration inside the solid, and a mass transfer coefficient.[10] Accordingly, increasing the S/F ratio enhances the concentration gradient between the cell interior and exterior, thereby increasing the driving force and diffusion rate. However, in the case of UAE kinetics, higher S/F ratios result in lower cavitation energy densities per unit volume available for extraction.[44]

Furthermore, once equilibrium in the extraction process is reached, increasing the S/F no longer improves extraction efficiency. In other words, the proportion of solvent to feed has no significant effect on diffusivity or the diffusion rate. At this stage, higher S/F ratios merely produce more diluted extracts. In addition to being unnecessary from a mass transfer standpoint, more diluted extracts also increase downstream concentration costs,[45,46,47] when optimizing the extraction of phenolics from pomegranate peel using a combined ultrasound-microwave-assisted approach, reported that the solvent-to-solid ratio significantly influenced yield and TPC values. An increase in the ratio from 30 to 50 mL g^{-1} improved extraction yield. However, further increases beyond 50 mL g^{-1} led to reduced yields. Similarly, Shijarath *et al.*[48] observed an optimal solvent-to-solid ratio for phenolic extraction from pomegranate peel, beyond which excessive dilution limited the driving force for mass transfer.

3.3 Initial extraction rates and driving forces

To quantify these observations, kinetic slopes were calculated and compared. During the very fast initial stage of extraction, observed for all processes, the slope of the cumulative extraction curve (mg GAE per g *vs.* min) was determined from the origin up to the point corresponding to approximately 80% of the total phenolic recovery and used as an estimate of the initial extraction rate. This slope, obtained by fitting a first-order equation, can be interpreted as the derivative of concentration with respect to time $\left(\frac{dC}{dt}\right)$, representing an apparent kinetic coefficient associated

Table 2 Apparent kinetic coefficients and R^2 values for the initial rapid extraction phase of phenolic compounds from pomegranate peel at different S/F ratio[a]

S/F ratio	Kinetic	Mean coefficient	R^2
5	SLE	0.1585 ± 0.0004	0.9079
5	UAE	0.2556 ± 0.0019	0.9520
10	SLE	0.2572 ± 0.0019	0.9371
10	UAE	0.2750 ± 0.0023	0.9275
30	SLE	0.3576 ± 0.0175	0.9054
30	UAE	0.3696 ± 0.0056	0.8869

[a] S/F: solvent/feed mass ratio; SLE: stirred liquid extraction; UAE: ultrasound-assisted extraction.

with the mass-transfer-controlled extraction stage. The same number of data points was used to calculate the slopes for both duplicates, ensuring comparability.

Table 2 reports the mean values of these apparent kinetic coefficients, along with their respective coefficients of determination (R^2). The R^2 values (~0.90) confirm that this fast initial extraction stage is adequately described by a linear model. Comparative analysis shows that increasing the S/F enhances the apparent kinetic coefficient for both SLE (0.1582 < 0.2572 < 0.3575, for S/F ratio of 5, 10, and 30, respectively) and UAE processes (0.2555 < 0.2750 < 0.3695).

Differences between the SLE and UAE processes are more clearly visualized in Fig. 6 alongside the data in Table 2. As the S/F ratio increases, the difference between the apparent kinetic coefficients of the two processes decreases. This behavior suggests that increasing the amount of solvent enhances the concentration gradient between the plant matrix and the extracting medium, thereby promoting compound diffusion. Consequently, the effect of ultrasound tends to be partially offset, as the extraction process becomes predominantly governed by diffusive flux. Thus, the concentration gradient emerges as a key factor in determining the efficiency of phenolic compound extraction from pomegranate peel flour.

Pomegranate peel is particularly rich in phenolic compounds, which may occur in free form or in less accessible bound, esterified, glycosylated, or insoluble forms. Free phenolic compounds are more readily extracted, whereas bound forms are better recovered through emerging technologies that disrupt the cellular microstructure. In the present study, even during the final stages of extraction with solvent replacement, high intensity ultrasound did not enhance the extraction rate. These results suggest that most phenolic compounds in pomegranate peel are easily extractable, which is consistent with previous findings.[49]

3.4 Modeling extraction kinetics with Peleg's model

Reducing the S/F ratio served as an alternative to approximate the SLE and UAE processes to a continuous, differential-level extraction. PLE is inherently a continuous process that can be interpreted at the differential scale, since the solvent comes into slow and constant contact with the plant matrix over time. In this process, small local concentration gradients are established between the matrix and the solvent. As the solvent percolates through the sample, extraction occurs progressively and directionally, resulting in mass transfer that proceeds in a continuous manner. Therefore, the extraction kinetics of the PLE process were also evaluated to provide a better understanding and comparison with the other extraction methods.

Peleg's model was applied to enable a more consistent comparison of the kinetic behaviors of the SLE and UAE processes with that of PLE. For the modeling, the mean values of the duplicate experiments for each process were used. The kinetic constants K_1 and K_2 were determined using R software. After estimating the initial concentrations, the initial concentrations for all SLE and UAE kinetics were equal to zero for all S/F ratio. In contrast, the initial concentration estimated for the PLE method

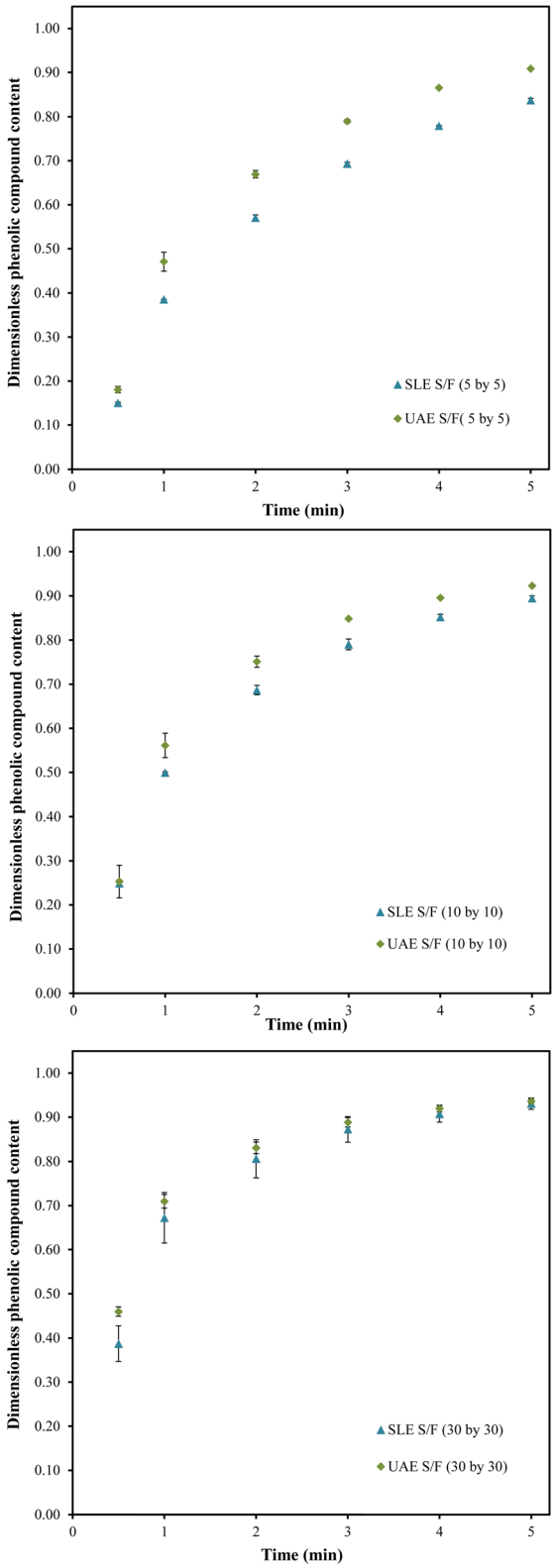

Fig. 6 Comparison of SLE and UAE dimensionless extraction kinetics at S/F ratio of 5, 10, and 30. S/F: solvent/feed mass ratio; SLE: stirred liquid extraction; UAE: ultrasound-assisted extraction.

was 14.7 mg GAE per g of flour. The kinetic curves modeled using Peleg's equation, along with the corresponding experimental data for the SLE, UAE, and PLE methods, are presented in Fig. 7.

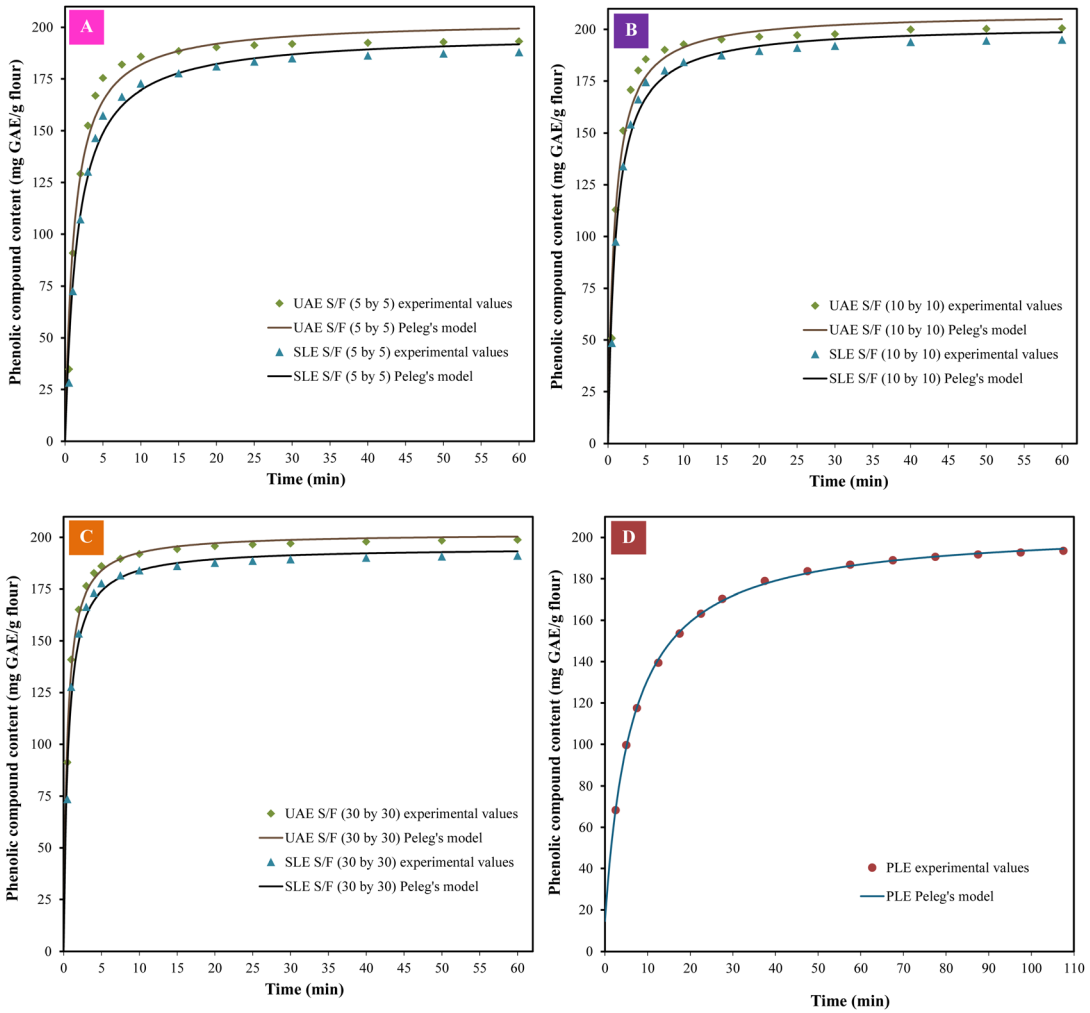

Fig. 7 Experimental extraction kinetics (symbols) and model-fitted curves (solid lines) based on Peleg's model for phenolic recovery under different extraction conditions: (A) SLE and UAE at S/F (5 by 5); (B) SLE and UAE at S/F (10 by 10); (C) SLE and UAE at S/F (30 by 30); and (D) PLE. S/F: solvent-to-feed mass ratio; SLE: stirred liquid extraction; UAE: ultrasound-assisted extraction; PLE: pressurized liquid extraction.

The estimated values for the constants K_1 and K_2 and their reciprocals B_0 and C_e, as well as the coefficients of determination (R^2), root mean square error (RMSE), and residual standard deviation (σ), are presented in Tables 3 and 4.

When comparing the SLE and UAE methods individually and considering increasing S/F ratio, it is evident for both that higher S/F values resulted in faster initial extraction rates, as indicated by lower K_1 values. For the same S/F ratio, the UAE method exhibited lower K_1 values compared to SLE, reflecting faster

Table 3 Estimated kinetic parameter K_1 from Peleg's model and its reciprocal B_0 for SLE, UAE, and PLE methods at different S/F ratio

S/F ratio	Method	K_1 estimate[a]	R^2	RMSE	Sigma	B_0[b]
5	SLE	0.00818	0.983	6.00	6.70	122.26
5	UAE	0.00580	0.963	8.61	9.62	172.40
10	SLE	0.00522	0.981	5.57	6.22	191.61
10	UAE	0.00417	0.958	8.28	9.26	239.71
30	SLE	0.00313	0.976	4.76	5.32	319.63
30	UAE	0.00245	0.984	3.54	3.96	408.79
—	PLE	0.03332	0.999	0.81	0.91	30.02

[a] K_1: constant related to the initial extraction rate (min g flour per mg GAE). [b] B_0: initial extraction rate constant at $t = 0$ (mg GAE per g flour min). S/F: solvent/feed mass ratio; SLE: stirred liquid extraction; UAE: ultrasound-assisted extraction; PLE: pressurized liquid extraction.

Table 4 Estimated kinetic parameter K_2 from Peleg's model and its reciprocal C_e for SLE, UAE, and PLE methods at different S/F ratio

S/F ratio	Method	K_2 estimate[a]	R^2	RMSE	Sigma	C_e[b]
5	SLE	0.00508	0.983	6.00	6.70	196.89
5	UAE	0.00492	0.963	8.61	9.62	203.25
10	SLE	0.00495	0.981	5.57	6.22	202.13
10	UAE	0.00481	0.958	8.28	9.26	207.94
30	SLE	0.00512	0.976	4.76	5.32	195.17
30	UAE	0.00495	0.984	3.54	3.96	202.01
—	PLE	0.00525	0.999	0.81	0.91	205.13

[a] K_2: capacity constant, which governs the approach of the yield toward its maximum value (g flour per mg GAE). [b] C_e: maximum extraction capacity (mg GAE per g flour). SLE: stirred liquid extraction; UAE: ultrasound-assisted extraction; PLE: pressurized liquid extraction.

extraction during the initial stages. This behavior is expected due to the effects of acoustic cavitation, enhanced turbulence, and localized thermal phenomena promoted by high-intensity ultrasound technology, which increase solvent accessibility to target compounds. However, the difference in K_1 between UAE and SLE decreased as the S/F ratio increased, suggesting that the concentration gradient becomes the dominant driving force in the extraction processes. These findings are consistent with the slope analysis of the initial kinetic points. The K_2 values were very similar between SLE and UAE, regardless of the S/F ratio, indicating that both techniques tend to achieve comparable final yields, despite exhibiting different extraction dynamics.

Regarding the PLE method, the kinetic coefficient K_1 was higher than in the other methods, indicating a lower initial extraction rate. However, the maximum extraction yield achieved was like those of SLE and UAE. In PLE, a smaller volume of solvent is enriched in the initial stages, unlike in SLE and UAE, where a larger and fixed mass of solvent is used from the start. Consequently, the instantaneous S/F ratios during the early stages of PLE are much lower, resulting in a reduced initial extraction rate. On the other hand, because fresh solvent continuously comes into contact with the matrix, the chemical potential difference remains at its maximum. As a result, despite the lower initial rate, phenolic compound recovery becomes efficient over time as the total volume of solvent increases.

3.5 Cumulative S/F and process efficiency

The total extraction time for the PLE method was longer than for the other methods for the total S/F of the process to reach a value of 100. Fig. 8 exhibits a comparison of the extraction methods with respect to cumulative S/F. To aid interpretation, a target concentration of 150 mg GAE per g (blue line), representing at least 80% of the total phenolic recovery for all processes, was selected. For this concentration, PLE required a total S/F of 16 and a processing time of 17.5 min. In contrast, UAE at S/F 5 by 5, 10 by 10, and 30 by 30 required approximately 3 min (S/F ≈ 20), 1.5 min (S/F ≈ 30), and 1–1.5 min (S/F ≈ 70),

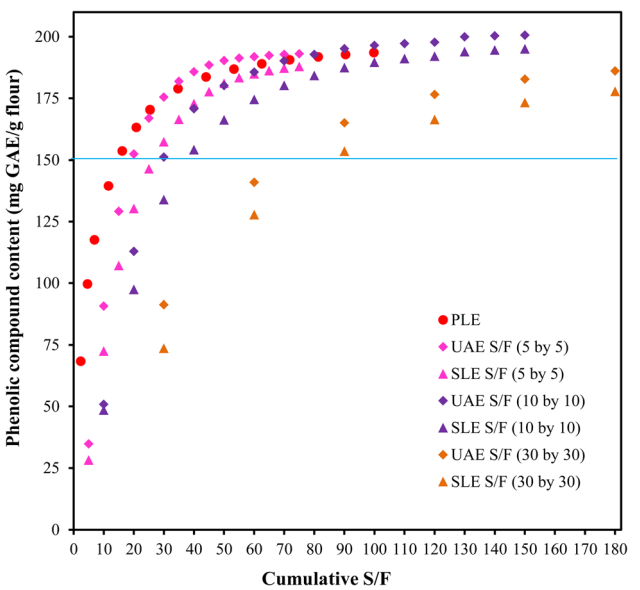

Fig. 8 Comparison of SLE, UAE, and PLE performance based on phenolic recovery and cumulative S/F. S/F: solvent/feed mass ratio; SLE: stirred liquid extraction; UAE: ultrasound-assisted extraction; PLE: pressurized liquid extraction.

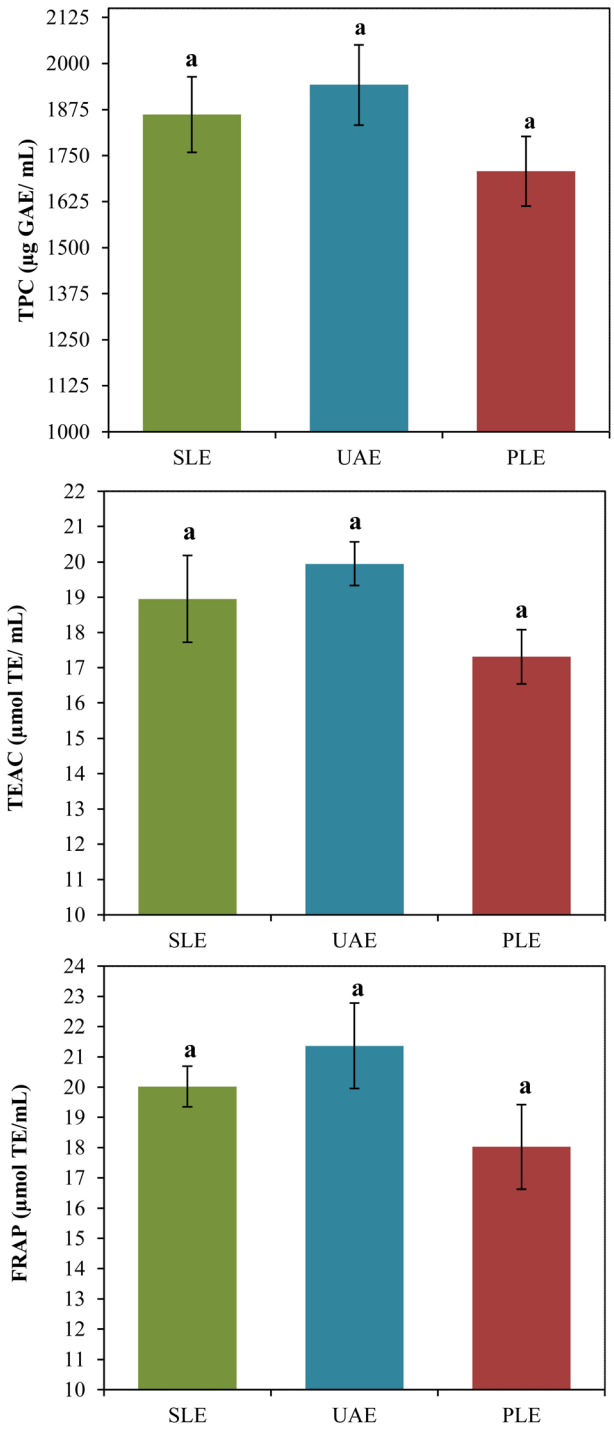

Fig. 9 Comparison of total phenolic content (TPC) and antioxidant activity (FRAP and TEAC) in representative extracts obtained by SLE, UAE, and PLE. SLE: stirred liquid extraction; UAE: ultrasound-assisted extraction; PLE: pressurized liquid extraction. Bars sharing the same letter ("a") do not differ significantly (Tukey's test, p-value >0.05).

respectively. For SLE at S/F 5 by 5, 10 by 10, and 30 by 30, the same concentration required about 4 min (S/F ≈ 27), 2 min (S/F ≈ 40), and 1.5 min (S/F ≈ 90), respectively.

Initially, PLE stands out for its lower solvent requirement. However, it demands a longer processing time. For the same total S/F of 100, the UAE process at 10 by 10 ratio outperformed PLE in yield while operating in a significantly shorter time (20 min *vs.* 107.5 min). Moreover, UAE provided both shorter processing times and lower solvent usage compared to SLE for achieving the 150 mg GAE per g concentration. These observations should be considered in process design to balance solvent and time efficiency with the need for extract concentration.

Using cumulative S/F as a common yardstick reveals complementary optima: PLE minimizes solvent at the cost of time; UAE reaches target TPC rapidly but can over-dilute if S/F is not capped. Hence, process synthesis should balance solvent duty, residence time, and downstream concentration energy, rather than targeting a single 'maximum yield' point.

3.6 Representative extracts

Fig. 9 shows the results for TPC and antioxidant activity of the representative phenolic extracts. The TPC of the representative extracts did not differ significantly among the extraction methods (p-value = 0.212). The mean concentration of phenolic compounds was 1836.88 ± 119.16 μg GAE per mL, which is consistent with the phenolic content observed in the extraction kinetics. Thus, for the same solvent consumption (total S/F = 100), the extraction techniques yielded similar TPC values. Antioxidant activity, assessed by TEAC and FRAP assays, also demonstrated comparable bioactive potential among extracts obtained by different methods, with no significant differences (TEAC, p-value = 0.132; FRAP, p-value = 0.148). The mean antioxidant activities were 18 947.47 ± 1330.92 μmol TE mL^{-1} (TEAC) and 19 805.13 ± 1683.69 μmol TE mL^{-1} (FRAP). However, the time required to obtain extracts with similar characteristics was approximately five times greater for PLE (107.5 min) compared to SLE and UAE (20 min).

Table 5 presents the quantification of selected phenolic compounds in pomegranate peel extract. When compared to the TPC, about 37% of phenolics were identified by HPLC-DAD analysis. Except for the flavonoid astragalin, the quantified phenolics did not differ significantly across extraction methods. Punicalagin and ellagic acid, in their various forms, were the predominant compounds. Nevertheless, pomegranate peel is rich in a wide diversity of phenolics, many of which are characteristic of the peel but were not quantified in this study. These include granatin, punicalin, and peduncalagin. In a previous exploratory study with the same raw material, tentative identification of phenolics in the hydroalcoholic extract of pomegranate peel flour included punicalin, punicalagin, gallocatechin, glucogallin, gallic acid, peduncalagin, granatin B, ellagic acid, ellagic acid deoxyhexoside, and salicylic acid.[50]

Russo *et al.* (2018)[51] quantified most of the compounds identified in the present study. However, in comparison, they reported lower levels of punicalagin A and B and higher levels of other compounds. They also quantified peduncalagin, granatin A, and catechin. Consistent with the present results, punicalagin and ellagic acid were the major compounds. These compounds are commonly quantified in pomegranate peel extracts, and higher levels of punicalagin have been reported in several studies (Kazemi *et al.*, 2016; Feng *et al.*, 2022; Liu *et al.*, 2022).[2,52,53]

3.7 Impact of extraction techniques on the microstructure of pomegranate peel flour

Fig. 10 presents scanning electron micrographs of pomegranate peel flour before and after extraction by SLE, UAE, and PLE. Initially, the raw material appears well preserved, with low porosity (Fig. 10A). After SLE (Fig. 10B), surface erosion is observed, evidenced by the presence of pores. These changes are consistent with the gradual solvent penetration and diffusion of target compounds during mass transfer-driven extraction processes.

In the sample subjected to UAE (Fig. 10C), the mechanical effects of acoustic cavitation are clearly visible. The surface of the flour exhibits delaminated and scratched regions, smoothed areas, and superficial erosions, indicating the localized action of shear forces and microjets. These effects are associated with enhanced initial extraction rates due to more accessible solvent pathways to the compounds of interest.[54]

Table 5 Phenolic compounds content (μg mL^{-1} extract) in representative pomegranate peel extracts obtained by SLE, UAE, and PLE

Phenolic compounds content (μg mL^{-1} extract)	SLE	UAE	PLE
Galloyl-glucoside	2.07 ± 0.07[a]	2.05 ± 0.11[a]	1.83 ± 0.06[a]
Digalloyl-HHDP-glucoside	45.84 ± 3.54[a]	46.47 ± 1.42[a]	42.54 ± 3.41[a]
Punicalagin A	208.55 ± 12.4[a]	200.96 ± 8.17 [a]	201.07 ± 2.87[a]
Punicalagin B	412.45 ± 42.5[a]	405.32 ± 2.4[a]	404.13 ± 15.5[a]
Ellagic acid-glucoside	32.74 ± 1.91 [a]	32.33 ± 0.8[a]	28.4 ± 3.97[a]
Ellagic acid-arabinoside	19.62 ± 1.42 [a]	19.31 ± 0.33[a]	17.57 ± 2.27[a]
Ellagic acid	21.78 ± 1.34[a]	21.34 ± 0.18 [a]	19.17 ± 2.31[a]
Quercetin-3-O-rutinoside (rutin)	1.28 ± 0.09[a]	1.33 ± 0.07[a]	1.06 ± 0.05[a]
Kaempferol-3-O-rutinoside (nicotiflorin)	1.39 ± 0.09[a]	1.32 ± 0.01[a]	1.27 ± 0.05[a]
Kaempferol-3-O-glucoside (astragalin)	1.58 ± 0.04[a,b]	1.6 ± 0.02[a]	1.45 ± 0.03[a,b]

[a] Means ± standard error. [b] Means followed by different letters (a and b) in the row differ significantly according to Tukey's test at a 5% significance level. SLE: stirred liquid extraction; UAE: ultrasound-assisted extraction; PLE: pressurized liquid extraction.

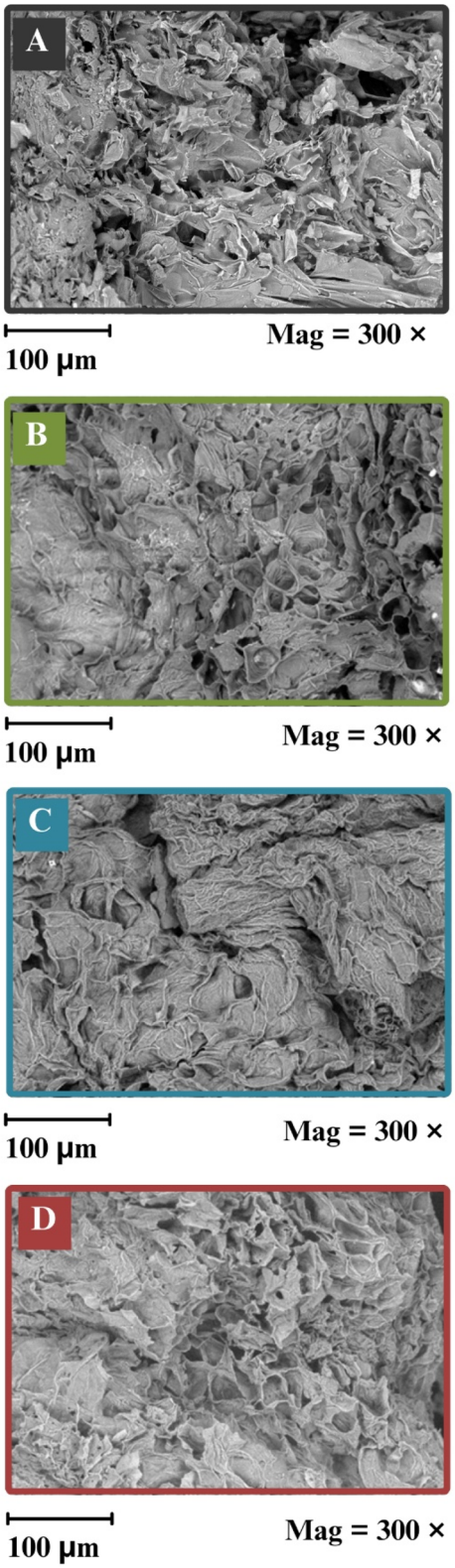

Fig. 10 Scanning electron micrographs of pomegranate peel flour: (A) raw material; (B) after stirred liquid extraction (SLE); (C) after ultrasound-assisted extraction (UAE); (D) after pressurized liquid extraction (PLE).

After the PLE process (Fig. 10D), the biomass structure presents more pronounced porosity and evident internal erosions. These effects may be attributed to the percolation of pressurized solvent throughout the matrix, promoting more efficient penetration. In addition, the moderate temperature used contributes to cell wall softening and improves solvation of the target compounds. This condition favors a more progressive and homogeneous extraction throughout the particle bed.[55,56]

3.8 Sustainability evaluation of the extraction processes *via* Path2Green

The sustainability of phenolic compound extraction processes using different techniques (SLE, UAE, and PLE) was assessed through the Path2Green metric, with results presented in Fig. 11. The 12 principles of sustainability are represented by colored icons, whose shades reflect the degree of alignment of each process with the respective principle. Green indicates strong adherence, yellow represents neutral performance, and red indicates low conformity. Lighter or darker shades reflect, respectively, lower or higher intensity in the evaluation.

The principles of biomass, solvent, purification, post-treatment, and application showed good alignment with sustainability. Pomegranate peel, the agro-industrial residue used as biomass in this study, is valorized as a raw material, promoting byproduct utilization and contributing to the overall sustainability of the process. The pretreatment of the biomass consisted exclusively of physical operations (drying and milling), which resulted in a score of −0.20. The solvents employed (water and ethanol) are considered green and are recommended by the Path2Green metric. The extracts obtained were scored with the highest rating for the principles of purification and post-treatment, as they are ready for use without requiring additional processing steps. Regarding the application principle, the extracts also demonstrated satisfactory performance, given their potential for use in the pharmaceutical, cosmetic, food, hygiene, and cleaning industries, as well as their function as natural additives. The transportation principle was positively evaluated, considering that the proposed biorefinery is more viable when located near juice and by-product industrial hubs, optimizing logistics and pomegranate peel residue utilization.

On the other hand, the principles of yield, resource reuse, and waste management did not achieve satisfactory scores. This is attributed to the fact that the study addresses only the initial stage of a potential biorefinery and does not yet include sequential extractions aimed at recovering other valuable compounds, such as biopolymers. Additionally, the solvents and inputs used were not recovered or reused during the processes.

Energy consumption was assessed based on the total extraction time for each kinetic, resulting in a score of −0.50 for all three methods, classified as high renewable energy use. However, for a cumulative S/F ratio of 100, both SLE and UAE processes (in the S/F 10 by 10 configuration) reached yields comparable to the PLE process, while requiring approximately

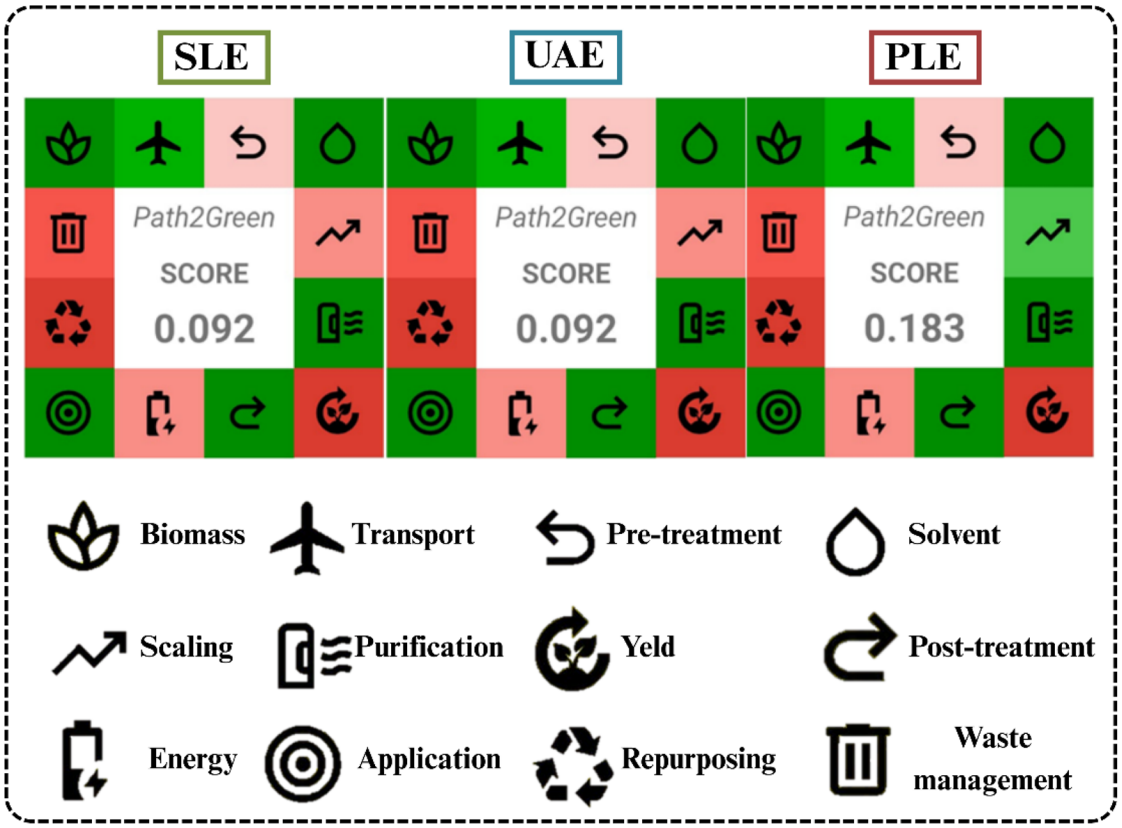

Fig. 11 Sustainability profile of SLE, UAE, and PLE according to the 12 principles of green extraction using the Path2Green metric. SLE: stirred liquid extraction; UAE: ultrasound-assisted extraction; PLE: pressurized liquid extraction.

five times less extraction time. This highlights an operational advantage for SLE and UAE under this specific condition.

As for scalability, the PLE method obtained a score of 0.50 due to its semicontinuous operation, while SLE and UAE, classified as automated batch processes, received lower scores (−0.50). Although final scores were influenced by this criterion, the individual analysis of each principle provides a detailed understanding of the opportunities and limitations of each process in the context of sustainability. This perspective is essential for guiding future improvements in process design.

4. Conclusions

This study provides new mechanistic insights into the role of PEF pretreatment in the extraction of phenolic compounds from pomegranate peel, revealing that the enhancement of mass transfer is not solely determined by membrane permeabilization. Despite achieving near-complete cell disintegration, the application of PEF prior to PLE resulted in only marginal improvements in phenolic yield. This outcome indicates that, in matrices with inherently high concentrations of soluble phenolics, such as pomegranate peel, the extraction process is predominantly governed by diffusion-driven mechanisms associated with the chemical potential difference between the matrix and the solvent, rather than by the removal of structural barriers alone. Comparative analyses using SLE, UAE, and PLE confirmed that more than 80% of total phenolics were recovered within the first 5 minutes of batch processes, and that increasing solvent availability diminished the relative contribution of acoustic cavitation-induced effects.

Kinetic modeling and cumulative S/F analyses further demonstrated that solvent accessibility and solute concentration are the main drivers of mass transfer, while PLE provided advantages in terms of scalability and solvent efficiency. These findings shift the conventional understanding of how PEF contributes to extraction processes, emphasizing that its effectiveness is highly matrix-dependent and strongly influenced by the chemical environment of the system.

Sustainability assessment using the Path2Green metric demonstrated which principles were fulfilled and which were not. Overall, the valorization of pomegranate peel, solvent selection, and extract application showed strong alignment with sustainable practices. However, since the full biorefinery concept of pomegranate peel was not fully addressed in this work, principles related to yield and waste management remain limited. Taken together, these results not only advance the fundamental understanding of mass transfer in phenolic recovery but also provide actionable insights for the sustainable and scalable valorization of pomegranate peel in industrial applications.

Future studies should integrate sequential extraction approaches, solvent recycling, and downstream fractionation to further enhance the valorization potential of pomegranate peel in industrial applications.

Conflicts of interest

There are no conflicts to declare.

Data availability

All data supporting the findings of this study are included within the article. Additional datasets generated or analyzed during the current work are available from the corresponding author upon reasonable request.

Acknowledgements

This study was financed, in part, by the São Paulo Research Foundation (FAPESP), Brazil. Process Numbers: #2020/11255-3, #2023/01876-9, and #2024/15579-9. Eric Keven Silva thanks the Brazilian National Council for Scientific and Technological Development (CNPq, Process no. 312695/2025-0) for the Research Productivity Fellowship.

References

1 F. F. de Araújo, D. de Paulo Farias, I. A. Neri-Numa and G. M. Pastore, *Food Chem.*, 2021, **338**, 127535.
2 Y. Liu, K. W. Kong, D.-T. Wu, H.-Y. Liu, H.-B. Li, J.-R. Zhang and R.-Y. Gan, *Food Chem.*, 2022, **374**, 131635.
3 P. García, C. Fredes, I. Cea, J. Lozano-Sánchez, F. J. Leyva-Jiménez, P. Robert, C. Vergara and P. Jimenez, *Foods*, 2021, **10**, 203.
4 H. N. Rajha, A.-M. Abi-Khattar, S. El Kantar, N. Boussetta, N. Lebovka, R. G. Maroun, N. Louka and E. Vorobiev, *Innov. Food Sci. Emerg. Technol.*, 2019, **58**, 102212.
5 G. M. L. Faria and E. K. Silva, *J. Environ. Chem. Eng.*, 2024, **12**, 113078.
6 P. P. Singh and M. D. A. Saldaña, *Food Res. Int.*, 2011, **44**, 2452–2458.
7 L. E. N. Castro, W. G. Sganzerla, A. P. G. Silva, O. D. John, T. L. C. T. Barroso, M. A. Rostagno and T. Forster-Carneiro, *Phytochem. Rev.*, 2025, **24**, 2059–2086.
8 D. Gertenbach, *Functional Foods: Biochemical and Processing Aspects*, 2002, 2, pp. 331–366.
9 A. Özçelik, S. S. Turgut, E. Küçüköner and E. Karacabey, in *Extraction Processes in the Food Industry*, ed. S. M. Jafari and S. Akhavan-Mahdavi, Woodhead Publishing, 2024, pp. 17–44.
10 J. E. Cacace and G. Mazza, *J. Food Eng.*, 2003, **59**, 379–389.
11 R. G. Maroun, H. N. Rajha, E. Vorobiev and N. Louka, in *Handbook of Grape Processing By-Products*, ed. C. M. Galanakis, Academic Press, 2017, pp. 155–181.
12 G. C. Milanezzi and E. K. Silva, *Innov. Food Sci. Emerg. Technol.*, 2025, **106**, 104242.
13 F. J. Barba, O. Parniakov, S. A. Pereira, A. Wiktor, N. Grimi, N. Boussetta, J. A. Saraiva, J. Raso, O. Martin-Belloso, D. Witrowa-Rajchert, N. Lebovka and E. Vorobiev, *Food Res. Int.*, 2015, **77**, 773–798.
14 J. Raso, W. Frey, G. Ferrari, G. Pataro, D. Knorr, J. Teissie and D. Miklavčič, *Innov. Food Sci. Emerg. Technol.*, 2016, **37**, 312–321.
15 Z. Liu, E. Esveld, J.-P. Vincken and M. E. Bruins, *Food Bioprocess Technol.*, 2019, **12**, 183–192.
16 O. Gorte, N. Nazarova, I. Papachristou, R. Wüstner, K. Leber, C. Syldatk, K. Ochsenreither, W. Frey and A. Silve, *Front. Bioeng. Biotechnol.*, 2020, **8**, 575379.
17 L. P. Ferraz and E. K. Silva, *ACS Food Sci. Technol.*, 2025, **5**, 3229–3253.
18 N. S. M. Yusof, B. Babgi, Y. Alghamdi, M. Aksu, J. Madhavan and M. Ashokkumar, *Ultrason. Sonochem.*, 2016, **29**, 568–576.
19 P. H. Nguyen, *J. Chem. Phys.*, 2024, **161**, 064110.
20 M. D. Razola-Díaz, R. Sevenich, O. K. Schlüter, V. Verardo and A. M. Gómez-Caravaca, *Foods*, 2025, **14**, 368.
21 G. Ntourtoglou, F. Drosou, T. Chatzimitakos, V. Athanasiadis, E. Bozinou, V. G. Dourtoglou, A. Elhakem, R. Sami, A. A. Ashour, A. Shafie and S. I. Lalas, *Appl. Sci.*, 2022, **12**, 6219.
22 S. Carpentieri, G. Ferrari and G. Pataro, *Front. Sustain. Food Syst.*, 2022, **6**, 854968.
23 B. Martín-García, U. Tylewicz, V. Verardo, F. Pasini, A. M. Gómez-Caravaca, M. F. Caboni and M. Dalla Rosa, *Innov. Food Sci. Emerg. Technol.*, 2020, **64**, 102402.
24 E. Demir, S. Tappi, K. Dymek, P. Rocculi and F. Gómez Galindo, *Trends Food Sci. Technol.*, 2023, **139**, 104120.
25 K. Tzima, N. P. Brunton, J. G. Lyng, D. Frontuto and D. K. Rai, *Innov. Food Sci. Emerg. Technol.*, 2021, **69**, 102644.
26 L. Barp, A. M. Višnjevec and S. Moret, *Foods*, 2023, **12**, 2017.
27 K. Ameer, H. M. Shahbaz and J. H. Kwon, *Compr. Rev. Food Sci. Food Saf.*, 2017, **16**, 295–315.
28 P. R. Toledo-Merma, M. H. Cornejo-Figueroa, A. D. R. Crisosto-Fuster, M. M. Strieder, L. O. Chañi-Paucar, G. Náthia-Neves, H. Rodríguez-Papuico, M. A. Rostagno, M. A. A. Meireles and S. C. Alcázar-Alay, *Foods*, 2022, **11**, 1070.
29 F. H. ASAE, U. Committee and A. A. B. Engineers, *ASAE Standards*, ANSI/ASAE S, 2007, 424, pp. 662–665.
30 O. Rastorhuiev, A. Matys, A. Wiktor, K. Rybak, A. Lammerskitten, S. Toepfl, W. Schnäckel, E. Gondek and O. Parniakov, *Appl. Sci.*, 2024, **14**, 4561.
31 L. P. Ferraz and E. K. Silva, *ACS Omega*, 2025, **10**, 20277–20285.
32 V. L. Singleton and J. A. Rossi, *Am. J. Enol. Vitic.*, 1965, **16**, 144.
33 N. Milićević, P. Kojić, M. Sakač, A. Mišan, J. Kojić, C. Perussello, V. Banjac, M. Pojić and B. Tiwari, *Ultrason. Sonochem.*, 2021, **79**, 105761.
34 M. Peleg, *J. Food Sci.*, 1988, **53**, 1216–1217.
35 F. T. Borsoi, H. S. Arruda, L. M. Reguengo, I. A. Neri Numa and G. M. Pastore, *Food Chem.*, 2025, **483**, 144254.
36 R. Re, N. Pellegrini, A. Proteggente, A. Pannala, M. Yang and C. Rice-Evans, *Free Radic. Biol. Med.*, 1999, **26**, 1231–1237.
37 I. F. F. Benzie and J. J. Strain, *Anal. Biochem.*, 1996, **239**, 70–76.
38 L. M. de Souza Mesquita, L. S. Contieri, F. A. e Silva, R. H. Bagini, F. S. Bragagnolo, M. M. Strieder,

F. H. B. Sosa, N. Schaeffer, M. G. Freire, S. P. M. Ventura, J. A. P. Coutinho and M. A. Rostagno, *Green Chem.*, 2024, **26**, 10087–10106.
39 M. G. Ziagova, C. Mavromatidou, G. Samiotis and E. Amanatidou, *J. Food Process. Preserv.*, 2022, **46**, e16639.
40 E. Rrucaj, S. Carpentieri, M. Scognamiglio, F. Siano, G. Ferrari and G. Pataro, *Foods*, 2024, **13**, 1043.
41 D. Frontuto, D. Carullo, S. M. Harrison, N. P. Brunton, G. Ferrari, J. G. Lyng and G. Pataro, *Food Bioprocess Technol.*, 2019, **12**, 1708–1720.
42 L. Hssaini, R. Ouaabou, H. Hanine, R. Razouk and A. Idlimam, *Sci. Rep.*, 2021, **11**, 21266.
43 G. Pavón-Melendez, J. A. Hernández, M. A. Salgado and M. A. García-Alvarado, *J. Food Eng.*, 2002, **51**, 347–353.
44 Y. Liu, X.-R. She, J.-B. Huang, M.-C. Liu and M.-E. Zhan, *Food Sci. Technol.*, 2018, **38**, 286–293.
45 S.-J. Fan, X.-Y. Zhang, Y. Cheng, Y.-X. Qiu, Y.-Y. Hu, T. Yu, W.-Z. Qian, D.-J. Zhang and S. Gao, *Molecules*, 2024, **29**, 3266.
46 F. Brahmi, I. Mateos-Aparicio, A. Garcia-Alonso, N. Abaci, S. Saoudi, L. Smail-Benazzouz, H. Guemghar-Haddadi, K. Madani and L. Boulekbache-Makhlouf, *Antioxidants*, 2022, **11**, 1401.
47 N. Singh, S. Kumar and D. S. Patle, *Sep. Purif. Technol.*, 2025, **359**, 130681.
48 T. R. Shijarath, M. G, D. K. Sahoo and S. Abdullah, *Food Human.*, 2024, **3**, 100456.
49 Z. Gulsunoglu, F. Karbancioglu-Guler, K. Raes and M. Kilic-Akyilmaz, *Int. J. Food Prop.*, 2019, **22**, 1501–1510.
50 G. M. L. Faria and E. K. Silva, *J. Clean. Prod.*, 2025, **524**, 146480.
51 M. Russo, C. Fanali, G. Tripodo, P. Dugo, R. Muleo, L. Dugo, L. De Gara and L. Mondello, *Anal. Bioanal. Chem.*, 2018, **410**, 3507–3520.
52 M. Kazemi, R. Karim, H. Mirhosseini and A. Abdul Hamid, *Food Chem.*, 2016, **206**, 156–166.
53 Y. Feng, J. Lin, G. He, L. Liang, Q. Liu, J. Yan and Q. Yao, *Molecules*, 2022, **27**(15), 4796.
54 F. Chemat, N. Rombaut, A.-G. Sicaire, A. Meullemiestre, A.-S. Fabiano-Tixier and M. Abert-Vian, *Ultrason. Sonochem.*, 2017, **34**, 540–560.
55 M. Plaza and M. L. Marina, *TrAC, Trends Anal. Chem.*, 2023, **166**, 117201.
56 M. Alboofetileh, M. Rezaei, M. Tabarsa, M. Rittà, M. Donalisio, F. Mariatti, S. You, D. Lembo and G. Cravotto, *Int. J. Biol. Macromol.*, 2019, **124**, 131–137.